Polarization attraction using counter-propagating waves in optical fiber at telecommunication wavelengths

S. Pitois, J. Fatome and G. Millot

Institut Carnot de Bourgogne (ICB), UMR-CNRS 5209 / Université de Bourgogne
9 av. Alain Savary, 21078 Dijon, France
Tel : +33 3 80 39 59 82, Fax : +33 3 80 39 59 71
spitois@u-bourgogne.fr

Abstract: In this work, we report the experimental observation of a polarization attraction process which can occur in optical fibers at telecommunication wavelengths. More precisely, we have numerically and experimentally shown that a polarization attractor, based on the injection of two counter-propagating waves around 1.55µm into a 2-m long high nonlinear fiber, can transform any input polarization state into a unique well-defined output polarization state.

OCIS codes: (060.4370) Nonlinear optics, fibers ; (190.4370) Nonlinear optics, fibers ; (230.4320) Nonlinear optical devices

References and links

1. K. Cvecek, K. Sponsel, R. Ludwig, C. Schubert, C. Stephan, G. Onishchukov, B. Schmauss, G. Leuchs, "2R-Regeneration of an 80-Gb/s RZ-DQPSK Signal by a Nonlinear Amplifying Loop Mirror," IEEE Photon. Technol. Lett. **19** (3), pp. 146–148 (2007).
2. Sonia Boscolo, Sergei K. Turitsyn, Keith J. Blow, "Nonlinear loop mirror-based all-optical signal processing in fiber-optic communications," Opt. Fiber Technol. Available online 17 March 2008.
3. E. Ip, A. P. T. Lau, D. J. F. Barros, and J. M. Kahn, "Coherent detection in optical fiber systems, " Opt. Express **16**, 753-791 (2008).
4. E. Ciaramella, F. Curti and S. Trillo, "All-optical signal reshaping by means of four-wave mixing in optical fibers," IEEE Photon. Technol. Lett. **13**, 142–144 (2001).
5. P. Honzatko, A. Kumpera, and P. Skoda, "Effects of polarization dependent gain and dynamic birefringence of the SOA on the performance of the ultrafast nonlinear interferometer gate, " Opt. Express **15**, 2541-2547 (2007).
6. Y. Takahashi, A. Neogi, H. Kawaguchi, "Polarization dependent nonlinear gain in semiconductor optical amplifiers," J. Quantum Electron. **34**, 1660–1672, (1998).
7. J. P. Gordon and H. Kogelnik, "PMD fundamentals: Polarization mode dispersion in optical fibers", PNAS **97**, 4541-4550 (2000).
8. J. Garnier, J. Fatome, and G. Le Meur, "Statistical analysis of pulse propagation driven by polarization-mode dispersion," J. Opt. Soc. Am. B **19**, 1968-1977 (2002).
9. E. Heebner, R. S. Bennink, R. W. Boyd, and R. A. Fisher, "Conversion of unpolarized light to polarized light with greater than 50% efficiency by photorefractive two-beam coupling," Opt. Lett. **25**, 257-259 (2000).
10. S. Pitois, G. Millot, and S. Wabnitz, "Nonlinear polarization dynamics of counterpropagating waves in an isotropic optical fiber: theory and experiments, " J. Opt. Soc. Am. B **18**, 432-443 (2001).
11. S. Pitois, A. Sauter, and G. Millot, "Simultaneous achievement of polarization attraction and Raman amplification in isotropic optical fibers, " Opt. Lett. **29**, 599-601 (2004).
12. S. Pitois, A. Picozzi, G. Millot, H.R. Jauslin and M. Haelterman, "Polarization and modal attractors in conservative counterpropagating four-wave interaction," Europhys. Lett. **70**, 88-94 (2005).

1. Introduction

Repolarizing an arbitrarily polarized optical signal by means of a lossless and instantaneous interaction induced by a polarization-control pump-beam is a fundamental effect of great interest for telecommunication applications and signal processing systems. Such a phenomenon could be used for example to combat the polarization sensitivity of certain

#91998 - $15.00 USD Received 22 Jan 2008; revised 27 Mar 2008; accepted 28 Mar 2008; published 25 Apr 2008

devices such as Nonlinear Optical Loop Mirror [1,2], coherent detection [3], signal reshaping [4] or semiconductor optical amplifier (SOA) [5,6] or even to limit the impairments of polarization mode dispersion (PMD) occurring during the propagation at very high bit rates [7,8]. In 2000, Heebner *et al*. reported the design of such a nonlinear polarizer taking place in a photorefractive crystal which can convert in the visible domain an unpolarized signal beam into a linearly polarized light with essentially a unit efficiency [9]. This device constitutes what could be called a polarization attractor, in the sense that all input polarization configurations are transformed into a unique well-defined polarization state. In a previous study, we have also theoretically and experimentally identified a novel type of attraction process which takes place in an optical-fiber system pumped by two counter-propagating laser beams [10]. More precisely, we have shown that a circular polarization pump could act as a lossless polarization attractor for a signal beam propagating in the opposite direction. These preliminary experiments have been performed both in a spun isotropic fiber [10,11] and a bimodal fiber [12] but only in the visible region. In this work, we exploit these last results in order to design a fiber-based polarization attractor capable to operate at telecommunication wavelengths. By using commercially available fibers and lasers around $\lambda = 1550$ nm, we have experimentally shown that such a fiber polarization attractor can transform any input polarization state into a unique well-defined polarization state. Moreover, we have observed that the input signal polarization fluctuations are washed out from the system by transferring these fluctuations to the counter-propagating pump, in good agreement with theoretical predictions.

2. Experimental device

Figure 1 represents the experimental setup used to observe the polarization attraction process at telecommunication wavelengths. Two counter-propagating waves with identical peak powers, i.e. a pump wave (arm1) and a signal wave (arm2), are generated from a nanosecond laser emitting 10-ns nearly square pulses at a repetition rate of 1 kHz around 1550 nm. The spectral bandwidth of the laser was in the order of 0.4 nm, allowing us to work far bellow the Brillouin threshold. The pump and signal waves have identical power thanks to a 50/50 coupler. Two polarization controllers (PC1 and PC2) were used to control the states of polarization of both the pump and signal beams. Then, two circulators were inserted in order to inject the counter-propagating waves into a 2 m-long highly nonlinear fiber (HNLF) as well as to isolate and monitor the light emerging from each end of the fiber. Note that the opposite of our previous works [10,11] where a spun isotropic fiber was used, the fiber involved in this experiment is a commercially available standard HNLF from *OFS* which was measured to be quasi-isotropic and was just carefully straightened to prevent unwanted bending-induced birefringence. Indeed, we estimate that, for a few meters-long fiber, the residual birefringence Δn has to be less that 10^{-8}.

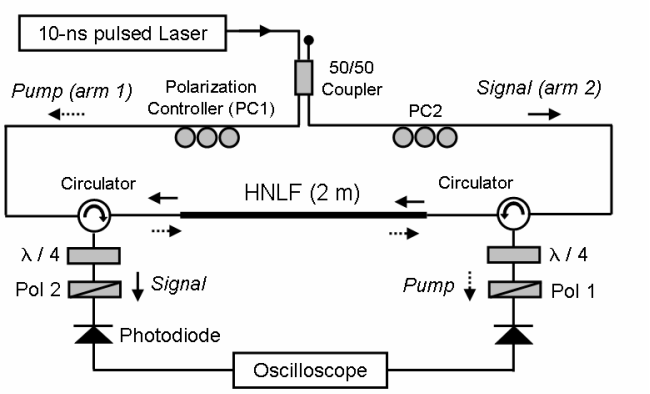

Fig. 1. Experimental set-up. HNLF : Highly Nonlinear Fiber, λ/4 : quaterwave-plate, Pol : Polarizer.

#91998 - $15.00 USD Received 22 Jan 2008; revised 27 Mar 2008; accepted 28 Mar 2008; published 25 Apr 2008

At one end of the fiber, we analyzed the polarization of the signal beam in the circular basis by means of a quarter-wave plate followed by a linear polarizer (Pol 2). Finally, the polarization controller PC1 was adjusted so that the polarization of the pump beam was as circular as possible whereas the signal was not fixed to a particular state and consequently possess an arbitrary polarization.

3. Theoretical evidences of the polarization attraction process

A system of two counter-propagating waves with arbitrary polarizations and propagating in an isotropic optical fiber can be described using the following nonlinear coupled equations:

$$\begin{aligned}
&\frac{\partial u}{\partial t}+\mathrm{v_g}\frac{\partial u}{\partial z}=i\frac{2}{3}\mathrm{v_g}\gamma\left[\left(|u|^2+2|v|^2\right)u+\left(2|\bar{u}|^2+2|\bar{v}|^2\right)u+2\bar{u}\,\bar{v}^{*}v\right]\\
&\frac{\partial v}{\partial t}+\mathrm{v_g}\frac{\partial v}{\partial z}=i\frac{2}{3}\mathrm{v_g}\gamma\left[\left(|v|^2+2|u|^2\right)v+\left(2|\bar{u}|^2+2|\bar{v}|^2\right)v+2\bar{v}\,\bar{u}^{*}u\right]\\
&\frac{\partial \bar{u}}{\partial t}-\mathrm{v_g}\frac{\partial \bar{u}}{\partial z}=i\frac{2}{3}\mathrm{v_g}\gamma\left[\left(|\bar{u}|^2+2|\bar{v}|^2\right)\bar{u}+\left(2|u|^2+2|v|^2\right)\bar{u}+2u\,v^{*}\bar{v}\right]\\
&\frac{\partial \bar{v}}{\partial t}-\mathrm{v_g}\frac{\partial \bar{v}}{\partial z}=i\frac{2}{3}\mathrm{v_g}\gamma\left[\left(|\bar{v}|^2+2|\bar{u}|^2\right)\bar{v}+\left(2|u|^2+2|v|^2\right)\bar{v}+2v\,u^{*}\bar{u}\right]
\end{aligned}\qquad (1)$$

In these equations, u and v are the amplitudes of the left and right circular components of the forward (pump) wave whereas $\bar{u}$ and $\bar{v}$ represent the amplitudes of the left and right circular components of the backward wave (signal). γ is the usual nonlinear Kerr coefficient and $\mathrm{v_g}$ is the group-velocity of light in the fiber. In the following, we will take $\gamma = 0.022\ \mathrm{m^{-1}W^{-1}}$ which corresponds to the experimental value of our HNLF. The first four terms on the right-hand sides of Eqs. (1) describe nonlinear phase modulations whereas the last term describes a resonant four-wave interaction responsible for energy exchanges between the two circular components of each wave. We would like to point out that both the total energy of each wave and the total energy along each polarization are conserved during the nonlinear interaction. A detailed theoretical description of the attraction process that takes place in the optical system described by Eqs. (1) is given in Ref [12] and one of the main results is that the circular polarization pump acts as an attractor for the signal polarization. Let us emphasize that this irreversible attraction process occurs thanks to two essential physical ingredients: the backward configuration of the interaction and the existence of a stable eigenmode of the system. Indeed, the counter-propagating configuration allows the signal polarization fluctuations to be continuously washed out from the system thanks to the transfer of polarization entropy between pump and signal waves. On the contrary, in the usual co-propagating geometry, the four-wave interaction is characterized by periodic analytical solutions describing a reversible exchange of energy between the waves, so that the forward configuration cannot support the existence of an attraction process. The second essential physical ingredient is the existence of a stable eigenmode of the equations governing the wave interaction. In the case of an isotropic fiber, this stable eigenmode consists of a mutual arrangement in which the two waves have identical circular polarizations. Accordingly, when one of the waves is injected into the nonlinear medium along one component of this eigenmode, the counter-propagating wave is then inevitably attracted to the other component of this eigenmode, regardless of its initial polarization state.

In the following, we will focus our attention on some novel numerical and experimental evidences of this original effect. In order to simulate the attraction process, we have numerically integrated Eqs. (1) using a standard split-step Fourier method. Due to the specific nature of counter-propagating interactions, propagation was resolved in time, i.e. at each step; the propagation was carried out from *t* to *t + dt*. The initial condition was therefore given for any *z* at *t = 0*. Finally, we have used super-Gaussian pulses close to the 10-ns experimental

#91998 - $15.00 USD Received 22 Jan 2008; revised 27 Mar 2008; accepted 28 Mar 2008; published 25 Apr 2008

pulses, instead of continuous waves, to avoid any numerical problem at the window boundaries. Figure 2(a) represents a series of numerical results for a pump beam having an input circular polarization state and for input signals with different elliptical polarizations.

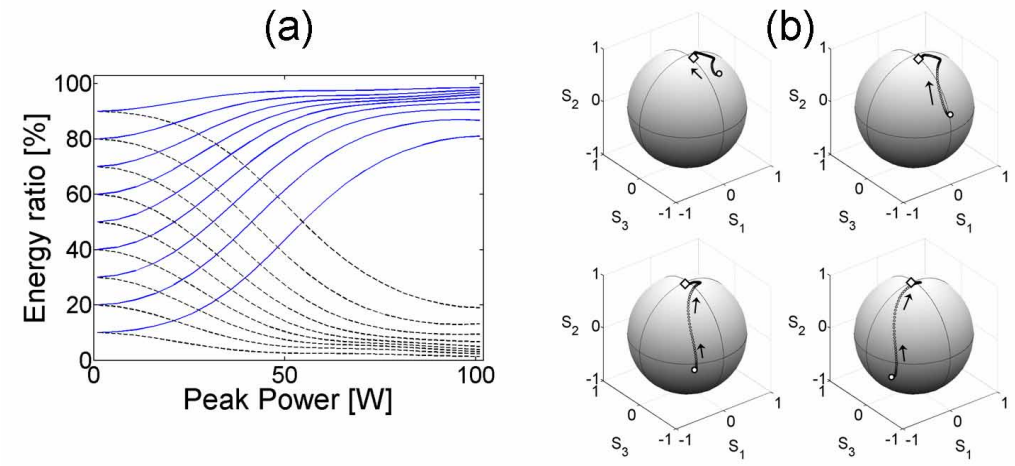

Fig. 2. Simulation results: (a) Evolution of the energy ratio contained in the right circular polarization (solid line) and in the left (dashed line) circular polarization as a function of the pump/signal power for different initial signal polarizations. (b) Evolution of the signal polarization state on the Poincaré sphere for four different input signal polarization states. The counter-propagating pump wave is injected with a right circular polarization ($S_2 = 1$).

For each input signal polarization, we have plotted in Fig. 2(a) the evolution of the output polarization state of the signal as a function of the pump and signal powers injected into the fiber. In order to represent the signal polarization in the circular basis ($|u|^2$, $|v|^2$), we have calculated the ratio of signal energy contained in the right circular polarization state (solid line) and in the left circular state (dashed line), respectively. We can clearly see in Fig. 2(a) that, any input signal polarization is attracted towards the right circular polarization imposed by the input pump polarization state. Even for the worst configurations, especially when the signal polarization is close to the left circular state, we can notice that more than 80% of the energy is repolarized towards the pump polarization state. Figure 2(b) completes the illustration of this attraction phenomenon by showing on the Poincaré sphere the evolution of the signal polarization state during its propagation through the optical fiber for four different input states. Let us recall that the Stokes vectors (S_1, S_2, S_3) used to represent any polarization state on the Poincaré sphere are defined by: $S_1 = i\, u^* v - i\, u v^*$, $S_2 = |u|^2 - |v|^2$ and $S_3 = u^*v+uv^*$. In our simulations, the Stokes vectors have been normalized with respect to $S_0 = |u|^2+|v|^2$, so that the radius of the Poincaré sphere is equal to unity. In Fig. 2(b), we have represented the evolution of the polarization state of the central part of the 10-ns signal pulse when a counter-propagating circularly-polarized pump beam ($S_2 = 1$) is injected into the fiber. Pump and signal input peak powers were fixed to 100 W. As can be seen, any input signal polarization converges asymptotically towards the right circular polarization state of the pump ($S_2 = 1$). Consequently, if the output signals are projected along the right-circular polarization by means of a polarizer, the resulting signal has a constant intensity, independently of the input polarization. This important repolarization capability underlines the great potential of the polarization attraction for various telecommunication applications.

4. Experimental results and telecommunication applications

Experimental evidences of this polarization attraction effect are shown in Fig. 3. In a same way that in the numerical simulations represented in Fig. 2(a), we have experimentally measured the ratio of the signal energy contained in the right circular polarization component (solid line) and in the left circular component (dashed line) for different input polarization

#91998 - $15.00 USD Received 22 Jan 2008; revised 27 Mar 2008; accepted 28 Mar 2008; published 25 Apr 2008

states (circles, triangles, squares and crosses) as a function of the input power and for a pump wave with a fixed right quasi-circular polarization (indeed, we have evaluated that the ratio of pump energy contained in the right circular polarization was 90 %). These results are presented in Fig. 3(a). As can be seen, when power increases, all input signal polarizations asymptotically converge to the same output polarization corresponding to the pump state (not perfectly right circular), and this independently of their initial states. These experimental results are in good agreement with theoretical predictions of Fig. 2(a), thus proving the efficiency of the attraction process.

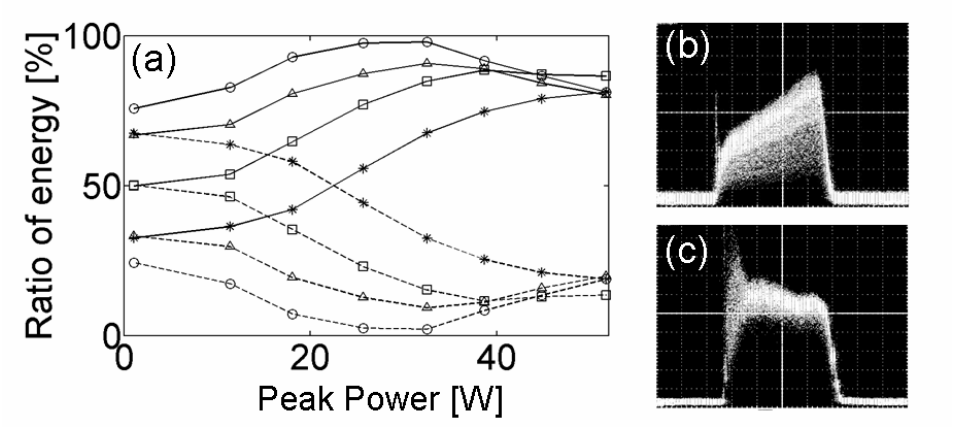

Fig. 3. (a). Experimental evolution of the energy ratio contained in the right (solid line) and in the left (dashed line) circular polarization as a function of the pump/signal power for four different initial signal polarization states. Output scrambled signal at P = 1 W (b) and at P = 45 W (c).

In order to illustrate the strong potential applications of this phenomenon into the telecommunication field, we have recorded several high persistence oscilloscope traces for different input powers. Figures 3(b) and 3(c) show the signals at the output of the fiber projected along the right-handed circular polarization component when the polarization of the input signal is scrambled at a low input power of 1 W (Fig. 3(b)) and at an input power of 45 W (Fig. 3(c)). We can clearly see that power fluctuations are greatly reduced when the power is sufficiently high to complete the attraction process (note that the slope observed in the temporal profile in Fig. 3(b) originates from the initial pulse outcoming from our nanosecond laser). This result proves the great potential of this polarization control technique for telecommunication applications, for example to minimize the polarization sensitivity of certain devices like non linear optical loop mirror or coherent detection or to combat the impairments of PMD. In order to complete the results represented in Figs. 3(b) and 3(c) and to better understand the dynamic of the attraction process between pump and signal waves, we have simultaneously recorded in Figs. 4(a) the pump and signal intensity profiles projected along the right-handed circular polarization component at both ends of the fiber at low and high powers. The polarization of the signal is scrambled at the fiber input while the pump wave is injected with a fixed right circular polarization at the other fiber end. For low pump and signal powers (1W), as expected in this linear propagation regime, no attraction phenomenon is observed : the output pump polarization remains constant (Fig. 4(a1)) whereas the output signal polarization (Fig. 4(a2)) exhibits strong fluctuations due to the scrambling process. At the opposite, as power is increased up to 45 W, the two counter-propagating waves are coupled through the nonlinear polarization and one can observe an efficient signal polarization attraction phenomenon as well as a spectacular transfer of the polarization fluctuations from the signal wave (Fig. 4(a4)) to the pump wave (Fig. 4(a3)). This effect has already been predicted theoretically in a previous work [12] but, to the best of our knowledge,

#91998 - $15.00 USD Received 22 Jan 2008; revised 27 Mar 2008; accepted 28 Mar 2008; published 25 Apr 2008

has never been experimentally observed. The strong signal intensity fluctuations are now significantly reduced compare to Fig. 4(a2) and a quasi-constant polarization state is obtained at the fiber output. As predicted by the theory presented in Ref. [12], these fluctuations are transferred to the pump wave which is now completely scrambled compare to Fig. 4(a1) so that the total polarization entropy of the system is conserved. These results are confirmed by the numerical simulations presented in Figs. 4(b) where we can clearly see this transfer of polarization fluctuations from the scrambled signal to the pump. Indeed, at low powers, 1W, (Fig. 4(b1) and 4(b2)), no attraction phenomenon is observed; the pump polarization is constant whereas the output signal keeps its strong fluctuations due to the scrambling process. On the other hand, for a signal and pump power of 45 W (Fig. 4(b3) and 4(b4)), a great signal polarization attraction process is observed as well as a complete transfer of polarization fluctuations from the signal to the pump wave.

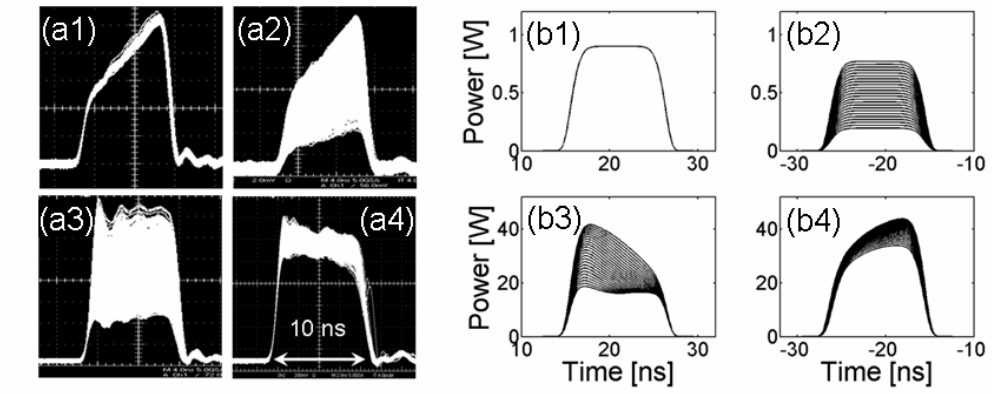

Fig. 4. Output pump (a1) and signal (a2) for P = 1 W after scrambling of the input signal polarization. Output pump (a3) and signal (a4) for P = 45 W after scrambling of the input signal polarization. (b1), (b2), (b3) and (b4) are numerical simulations corresponding Figs. (a1), (a2), (a3) and (a4), respectively.

5. Conclusions

In this work, we have reported the experimental observation and numerical modelling of a polarization attraction process in the usual telecommunication band around 1.55 μm. This attraction phenomenon was observed between two counter-propagating 10-ns waves injected into a 2-m long standard HNLF. We have also pointed out an experimental evidence of a striking polarization fluctuations exchange process occurring between the pump and the signal waves. We strongly believe that this universal repolarizer which is lossless, instantaneous and which can be coupled with Raman amplification [11] could therefore constitute a powerful tool to combat detrimental polarization effects in telecommunication and signal processing systems, for example to combat the polarization sensitivity of certain devices like non linear optical loop mirror or coherent detection or to combat the impairments of PMD which strongly limits the transmission distance in optical fibers-based telecommunication lines at very high bit rates. Nethertheless, we would like to emphasize that a critical challenge in the present system here is that high powers are required so that cw waves can actually not be used. We believe that in the future, very-highly nonlinear fibers, such as chalcogenide or bismuth fibers could be used so that the required powers could be compatible with usual telecommunication parameters.

Acknowledgment

We would like to acknowledge financial support of the Agence National de la Recherche (FUTUR project), the GDR PhoNoMi2 and the Conseil Regional de Bourgogne.

#91998 - $15.00 USD Received 22 Jan 2008; revised 27 Mar 2008; accepted 28 Mar 2008; published 25 Apr 2008